The role of gap plasmons in light emission from tunnel junctions

Shawn Divitt, Palash Bharadwaj, and Lukas Novotny*

ETH Zürich, Photonics Laboratory, 8093 Zürich, Switzerland

*lnovotny@ethz.ch

Abstract: Light emission from the junction of a scanning tunneling microscope (STM) is examined in the presence of 20 nm topographical features in thin gold films. These features significantly modify the emission rates of the junction. Contributions to this modification are discriminated by examining emission rates on samples where the material is varied spatially. It is found that the variability in STM photoemission rates between a gold tip and a gold sample under ambient conditions is due to the modification of localized gap plasmon modes and not to the presence of an electroluminescent gold cluster on the STM probe apex.

OCIS codes: (250.5403) Plasmonics; (240.7040) Tunneling; (300.2140) Emission.

References and links

1. Y. Zhang, E. Boer-Duchemin, T. Wang, B. Rogez, G. Comtet, E. L. Moal, G. Dujardin, A. Hohenau, C. Gruber, and J. R. Krenn, "Edge scattering of surface plasmons excited by scanning tunneling microscopy," Opt. Express **21**, 13938–13948 (2013).
2. P. Bharadwaj, A. Bouhelier, and L. Novotny, "Electrical excitation of surface plasmons," Phys. Rev. Lett. **106**, 226802 (2011).
3. T. Wang, E. Boer-Duchemin, Y. Zhang, G. Comtet, and G. Dujardin, "Excitation of propagating surface plasmons with a scanning tunnelling microscope," Nanotechnol. **22**, 175201 (2011).
4. S. Egusa, Y.-H. Liau, and N. F. Scherer, "Imaging scanning tunneling microscope-induced electroluminescence in plasmonic corrals," Appl. Phys. Lett. **84**, 1257–1259 (2004).
5. J. I. Gonzalez, T.-H. Lee, M. D. Barnes, Y. Antoku, and R. M. Dickson, "Quantum mechanical single-gold-nanocluster electroluminescent light source at room temperature," Phys. Rev. Lett. **93**, 147402 (2004).
6. D. Walmsley, T.-S. Tan, and P. Dawson, "Light emission from gold and silver thin films in a scanning tunneling microscope: role of contamination and interpretation of grain structure in photon maps," Surf. Sci. **572**, 497–520 (2004).
7. F. Silly, A. O. Gusev, A. Taleb, M.-P. Pileni, and F. Charra, "Single nanoparticle manipulation with simultaneously recorded STM-induced light emission," Mat. Sci. Eng. C **19**, 193–195 (2002).
8. K. Perronet, L. Barbier, and F. Charra, "Influence of the Au(111) reconstruction on the light emission induced by a scanning tunneling microscope," Phys. Rev. B **70**, 201405 (2004).
9. T. Uemura, M. Akai-Kasaya, A. Saito, M. Aono, and Y. Kuwahara, "Spatially resolved detection of plasmon-enhanced fluorescence using scanning tunneling microscopy," Surf. Interface Anal. **40**, 1050–1053 (2008).
10. D. Fujita, K. Onishi, and N. Niori, "Light emission induced by tunneling electrons from surface nanostructures observed by novel conductive and transparent probes," Microsc. Res. Techniq. **64**, 403–414 (2004).
11. L. Douillard and F. Charra, "High-resolution mapping of plasmonic modes: photoemission and scanning tunnelling luminescence microscopies," J. Phys. D **44**, 464002 (2011).
12. U. C. Fischer and H. P. Zingsheim, "Submicroscopic pattern replication with visible light," J. Vac. Sci. Technol. **19**, 881–885 (1981).
13. P. Nagpal, N. C. Lindquist, S.-H. Oh, and D. J. Norris, "Ultrasmooth patterned metals for plasmonics and metamaterials," Science **325**, 594–597 (2009).
14. M. G. Boyle, J. Mitra, and P. Dawson, "The tip-sample water bridge and light emission from scanning tunnelling microscopy," Nanotechnol. **20**, 335202 (2009).
15. P. Dawson and M. G. Boyle, "Light emission from scanning tunnelling microscope on polycrystalline Au films – what is happening at the single-grain level?" J. Opt. A: Pure Appl. Opt. **8**, S219 (2006).

#195365 - $15.00 USD Received 6 Aug 2013; revised 21 Sep 2013; accepted 23 Sep 2013; published 4 Nov 2013

16. R. Branscheid, V. Jacobsen, and M. Kreiter, "STM induced light from nontrivial metal structures: Local variations in emission efficiency," Surf. Sci. **602**, 176 (2007).
17. J. Mitra, L. Feng, M. G. Boyle, and P. Dawson, "Electromagnetic interaction between a metallic nanoparticle and surface in tunnelling proximity–modelling and experiment," J. Phys. D Appl. Phys. **42**, 215101 (2009).
18. M. G. Boyle, J. Mitra, and P. Dawson, "Infrared emission from tunneling electrons: The end of the rainbow in scanning tunneling microscopy," Appl. Phys. Lett. **94**, 233118 (2009).
19. J. Aizpurua, S. P. Apell, and R. Berndt, "Role of tip shape in light emission from the scanning tunneling microscope," Phys. Rev. B **62**, 2065–2073 (2000).
20. P. Johansson, R. Monreal, and P. Apell, "Theory for light emission from a scanning tunneling microscope," Phys. Rev. B **42**, 9210–9213 (1990).
21. D. W. Lynch and W. R. Hunter, "Comments on the optical constants of metals and an introduction to the data for several metals," in *Handbook of Optical Constants of Solids*, E. D. Palik, ed. (Academic, 1998), pp. 275–367.

1. Introduction

The use of scanning tunneling microscope (STM) probes to electrically excite surface plasmon polariton (SPP) modes has received recent attention [1]. It has been shown that the SPPs arise in this case from the decay of localized charge oscillations in the tip-sample gap, known as gap plasmons [2–4]. In a separate context it has been shown that electroluminescent metal clusters can be generated in electromigrated metal break-junctions [5], which are similar to STM junctions in that a tunneling barrier can be created in a spatially localized region. Further, it has been shown that photoemission rates from STM junctions can be highly variable and, during the raster-scan of a sample, line-to-line variations in the emission rate can be significant [6–10]. So far, there has been no study showing that such variations are always the result of a change in the tip-sample cavity, and therefore the gap plasmon mode structure, and not the result of spontaneously generated electroluminescent metal clusters attached to the STM probe/tip.

The purpose of the study presented in this paper is to controllably modify the photoemission rate of an STM tunnel junction and to understand the nature of this modification. In order to accomplish this goal, photoemission rate-variation events were generated between Au probes and three distinct sample types. This allowed for discrimination between emission from a gap plasmon and emission from a hypothetical "bright tip" on which an electroluminescent gold cluster has been excited at the apex of the STM probe. Experiments using three separate sample types were used to show that emission rate modification can be achieved and to elucidate the process from which the modification stems.

2. Experimental details

Experiments were performed using an inverted microscope and custom-built STM system. The microscope allowed for the collection of light emitted directly from gap plasmons as well as from SPPs and was similar in design to one previously published elsewhere [2]. The STM was placed in constant current mode and operated under ambient conditions. Electrochemically etched Au tips of radius ~50 nm were attached to a piezoelectric positioner and used as STM probes in each experiment. Au tips were chosen because photoemission rates are generally higher using Au than either PtIr or W tips and do not degrade as quickly as Ag tips [11]. Each sample was deposited onto a glass cover slip and light from the tip-sample junction region was collected through the sample and cover slip by an oil-immersion objective. The objective had a numerical aperture of 1.4 and operated under oil with a refractive index of 1.51. The collected light was imaged onto a thermoelectrically-cooled avalanche photodiode detector. During an experiment the sample was positively biased with respect to the probe, such that electrons tunneled from the probe to the sample, and raster-scanned (right to left, top to bottom) using a piezoelectric stage. Positive bias was chosen because it tends to have higher emission rates than negative bias. Topography and photoemission were simultaneously recorded for each scan.

#195365 - $15.00 USD Received 6 Aug 2013; revised 21 Sep 2013; accepted 23 Sep 2013; published 4 Nov 2013

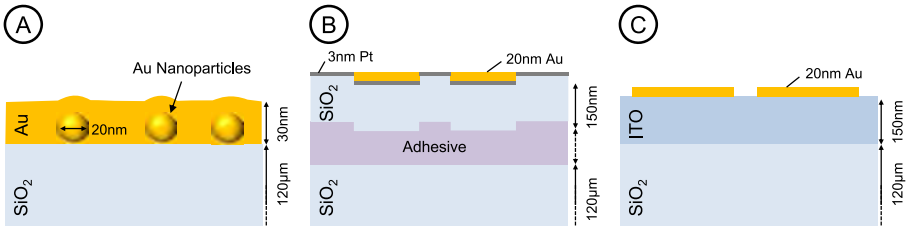

Fig. 1. Cross-sections of sample types A, B, and C as described in the text.

Experiments were made using three distinct sample types. Each type is displayed in Fig. 1.

Sample type A consisted of gold particles buried beneath an evaporated gold film. 20 nm diameter Au particles dispersed in water were spin coated at 3000 rpm onto a clean glass cover slip. The slip was then placed immediately into a vacuum chamber and a 30 nm Au film was deposited by thermal evaporation at 0.1 nm/second. This resulted in a continuous but partially transparent Au film with 20 nm topographical features spaced at approximately 1 feature per square micron.

Sample type B consisted of topography-free Au Fischer patterns [12] in a Pt matrix. These samples were produced using a Si wafer template-stripping method [13]. 200 nm polystyrene spheres suspended in water were spin-coated at 3000 rpm onto a clean silicon wafer chip. The sample was cleaned in oxygen plasma for 15 seconds at 200 W and immediately placed into a vacuum chamber. A 20 nm Au film was deposited by e-beam evaporation. The beads were then removed by vigorous ultrasonication in methanol and the chip was blown dry with nitrogen gas. The sample was again cleaned in oxygen plasma for 30 seconds at 200 W and placed into a vacuum chamber. 3 nm of Pt followed by 150 nm of SiO_2 was deposited by e-beam evaporation, each at 0.1 nm/second. The silicon chip was then glued to a glass cover slip using Norland 81 UV-curable adhesive (refractive index 1.56) and allowed to cure overnight under an 8 W UV lamp. After curing, the chip was cleaved from the cover slip using a razor blade and thereby a very flat Au-Pt surface (300-500 pm rms roughness as measured by tapping-mode AFM and STM) was revealed.

Sample type C consisted of Au Fischer patterns on indium tin oxide (ITO). 1.6 micron polystyrene beads were spin-coated at 3000 rpm onto a commercially produced ITO-coated cover slip, followed by Au deposition and ultrasonication similar to sample type B. This procedure leaves 20 nm high Au topographical features on ITO.

3. Results and discussion

The topographic and photoemission maps produced by a representative STM light emission experiment on sample type A are given in Figs. 2(a) and 2(c). Recorded light collection rates begin at approximately 10^4 counts per second as shown in Fig. 2(b). In order to stimulate a photoemission-rate variation event, the bias voltage was abruptly increased during scanning to a value of 4.5 V and then reduced back to 2.25 V. A tunneling bias of 4.5 Volts is unstable under ambient conditions and can lead to electrical breakdown of the air over the applicable distance scale of ~8 Angstroms. Accordingly, an instability is likely to lead to an event that affects the shape and/or the chemistry of the probe surface, which is typically enveloped in a water meniscus under ambient conditions [14] and may operate in the presence of surface adsorbates [6]. Such an event is viewable in each part of Figs. 2(a)-2(d) where an abrupt change in light emission corresponds to an abrupt change in apparent topography. From the topography cross-section given in Fig. 2(d) it is seen that for this particular case the probe either deformed

#195365 - $15.00 USD Received 6 Aug 2013; revised 21 Sep 2013; accepted 23 Sep 2013; published 4 Nov 2013

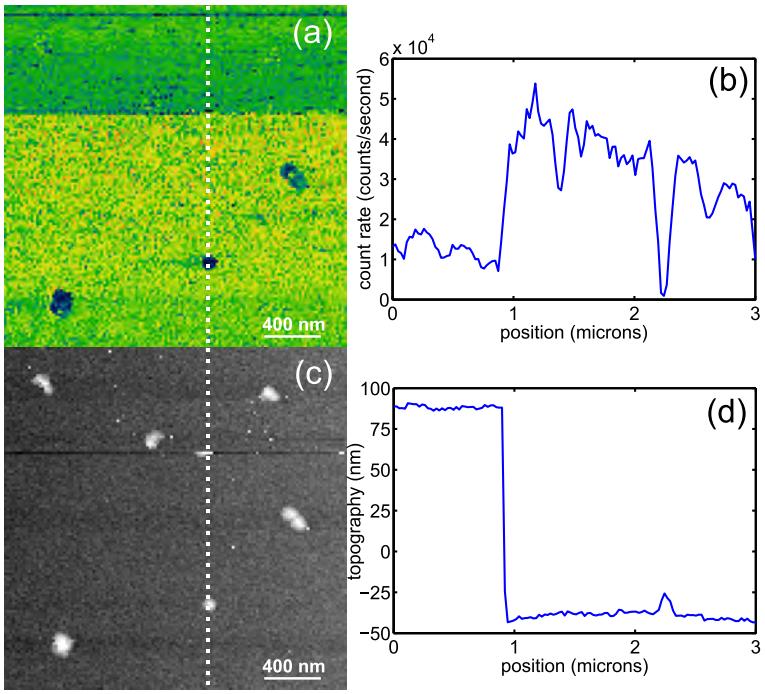

Fig. 2. (a) and (c) Simultaneous photoemission and topographical maps of a 3×3 micron area on sample type A. The map in (a) has been scaled logarithmically. The map given in (c) has been filtered such that the mean topographical height value of each line in the raw image has been subtracted individually to provide contrast between the bulk film and the embedded particle regions. (b) Photoemission-counts cross-section along the dashed line in a 3×3 point moving average of (a). (d) Topography cross-section along the dashed line in an un-filtered version of (c). The bright regions in (c) correspond to apparent locations of Au particles. The STM parameters were as follows: V_s = 2.25 V, I = 1 nA, sampling time per point was 30ms. Scan resolution was 128×128 points.

or lost material such that the piezoelectric positioner was required to extend by ~140nm in order to maintain tunneling contact. Accordingly, the photoemission rate increased on the flat film region by a factor of ~4 after the event. Furthermore, a very large emission rate contrast emerged between the flat film and the particles. On the buried particles the count rate became indistinguishable from dark count noise. Figure 2 also serves as an example of the typical behavior of a tip during a brightening event; a photoemission-rate increase is generated most often after a deformation or loss of material at the tip apex.

Sudden events that affect the photoemission rate are well documented in STM light-emission experiments [6]. After an event, the rate can increase for a period of time before rapidly decreasing, on the order of milliseconds, following a subsequent event or by slowly decreasing, on the order of minutes, in the absence of a specific event. Since events leading to photoemission variations must necessarily modify the characteristics of the probe, it could be that the probe itself is emitting light as a “bright tip” through the electrical excitation of electroluminescent gold clusters that are generated at the tip apex. Such clusters have been shown to exist in other circumstances and to electroluminesce by Gonzalez et al. [5]. They describe the clusters to be bright but unstable for a d.c. bias.

A luminescent cluster would need to be mechanically attached to the tip in order to generate

#195365 - $15.00 USD Received 6 Aug 2013; revised 21 Sep 2013; accepted 23 Sep 2013; published 4 Nov 2013

a photoemission map like the one shown in Fig. 2(a). This could theoretically be accomplished by a material which holds the cluster and is also attached to the tip, such as adsorbates or by non-metal sample materials. This material could also provide an electrical pathway to the cluster. Further, luminescence from the cluster is expected to be greatly quenched given its close proximity to the metal tip and sample. This is consistent with the data shown in Fig. 2. Emission in the hypothetical bright-tip area at the bottom of Fig. 2(a) has an electron-to-photon conversion efficiency of only $\sim 10^{-5}$.

Driven by this bright tip hypothesis, samples composed of two different metals were fabricated. A sample of type B, composed of topographically flat platinum and gold structures laterally-sized on the scale of 50 nm, would allow a bright tip to be differentiated from other radiative processes. Further, the presence of two materials side-by-side allows us to determine the true relative emission efficiency. In contrast, experiments where the sample material is mechanically swapped leaves room for changes to the STM probe during the interim and cannot reliably account for line-to-line emission changes without statistical arguments.

The fact that the sample is flat has important consequences for topographic and photoemission maps. As is well known in scanning probe microscopy, a topographic map is the result of the convolution between the tip and sample. For example, a sample with many needle-like spikes would result in a topographic image that looks like many identical versions of the tip shape. Consequently, the photoemission image has characteristics of the topographic image with respect to this convolution because the light emission stems from activity at the tip-sample junction. The three dimensional nature of both the tip and sample causes the interaction between them to occur at different points on the tip at different times depending on sample topography [15, 16].

A flat sample removes the effects of the tip shape on the topographic map, as compared to rough samples, in terms of the convolution. A flat sample has smaller excursions and as a result a much smaller area of the tip is sampled in the convolution. Simply, it is the last few atoms on the tip that determine the image and not a large portion of the tip. This leaves the true sample material layout to determine the photoemission map because the portion of the tip involved in the convolution is much more needle-like. As a consequence, the sample always interacts with the same part of the tip which would not be the case for rougher samples. However, a flat sample does not remove the dependence of light emission on the tip in terms of gap plasmon modes that can exist. The excited plasmon modes and emission intensity can depend strongly on the tip shape [17, 18].

Within the context of convolution and the bright tip hypothesis, the extreme change in apparent light emission rates at the position of particles after the brightening event in Figs. 2(a) and 2(b) can be interpreted. A theoretical bright cluster contains only tens of atoms [5]. Such a cluster would be very small and would occupy only an isolated region of the tip. As shown in Fig. 2(c) the tip has a diameter of approximately 75nm, after the abrupt change shown in Fig. 2(d), judging from the apparent lateral size of the 20 nm Au spheres in the image. Therefore, if a cluster is present on the tip and is positioned such that it receives current while on the flat film then it would stop receiving current, and go dark, as the tip traverses a protrusion. This is because the location on the tip through which current flows is changing due to the convolution effect. The current would only flow through the cluster when the tip and sample are correctly aligned and this would only occur in a small portion of the total apparent particle area in the photoemission map. Notice that, in Fig. 2(a), there appear to be very small bright regions present on the protrusions.

Continuing within the bounds of the bright tip hypothesis, Fig. 1 can be used to understand the expected behavior of a luminescent cluster on sample type B. The Pt film is only 3 nm thick and the Au features are 20 nm thick with a further 3 nm of Pt underneath. It bears noting that

#195365 - $15.00 USD Received 6 Aug 2013; revised 21 Sep 2013; accepted 23 Sep 2013; published 4 Nov 2013

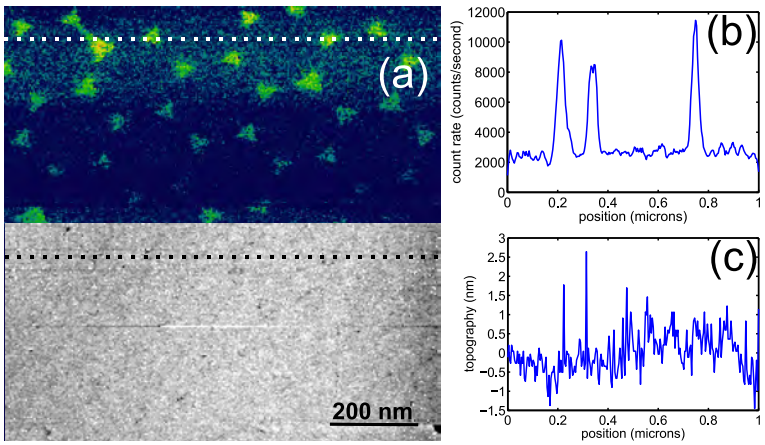

Fig. 3. (a) Simultaneous photoemission(top) and topographical(bottom) maps of a 1×1 micron area on sample type B. (b) Photoemission-counts cross-section along the dashed line in a 3×3 point moving average of (a,top). (c) Topography cross-section along the dashed line in (a,bottom). The triangular regions in (a,top) correspond to apparent positions of Au as deposited in a Fischer pattern in the sample. The remaining regions in (a,top) correspond to Pt. The STM parameters were as follows: V_s = 2.1 V, I = 0.7 nA, sampling time per point was 8ms. Scan resolution was 256×256 points.

that the work function of Pt and Au are similar at around 5 eV. This means that the tunneling barrier associated with a bright cluster would have essentially the same characteristics on both Pt and Au. Therefore, in a sample where the thickness and structure of Au and Pt is the same, the emission of a cluster is expected to be quite similar on both materials.

A typical photoemission and corresponding topographic map for a sample of type B is given in Fig. 3(a). While this map contains brightening events, the emission rate is clearly modulated by the sample material as shown in Fig. 3(b). This modulation is not accompanied by topographical changes, as shown in Fig. 3(c). In a bright tip scenario it is expected that the Au features should not be brighter than the Pt film. This is in view of the increased extinction, due to increased thickness, and scattering effects expected from the Au features. In Fig. 3(a) it is seen that the Au features are in fact brighter than the Pt film. Upon close inspection, the line-to-line changes in photoemission do not affect the emission ratio between gold and platinum, which is a factor 5 in this case. Experiments on sample type B were repeated with several tips on several samples at sample biases between 1.5 and 3 V and constant current set-points between 0.1 and 10 nA. Behavior consistent with the bright-tip hypothesis was never observed.

While this experiment does not lend support to the bright tip hypothesis, it does reinforce the existing theory [17, 19, 20] with respect to the presence of localized gap plasmon modes between the tip and sample. The imaginary part of the dielectric function of platinum near the typical STM light-emission wavelength of 700 nm is $\sim23\varepsilon_0$, which is a factor 18 larger than that of gold at that wavelength [21]. For this reason it is expected that plasmonic activity on the platinum is quenched relative to gold. This expectation is in agreement with the findings given in Fig. 3(b).

Although the findings of the Au-Pt experiment do not support a bright-tip hypothesis, neither is it necessarily precluded. If both a bright tip and a gap plasmon are present and emissive then it is difficult to discriminate between the two contributions. Therefore, samples of type C were used to differentiate between bright tip and gap plasmon contributions. Since a gap plasmon cannot exist on ITO, the presence of light emission on ITO would serve verify a bright tip.

#195365 - $15.00 USD Received 6 Aug 2013; revised 21 Sep 2013; accepted 23 Sep 2013; published 4 Nov 2013

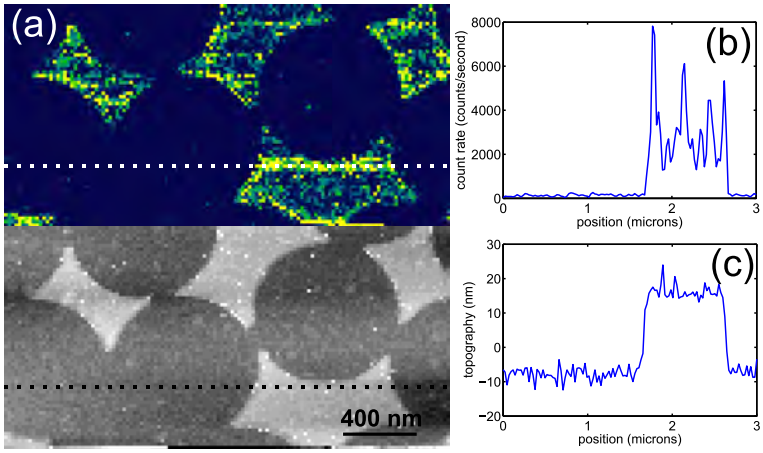

Fig. 4. (a) Simultaneous photoemission(top) and topographical(bottom) maps of a 3×3 micron area on sample type C. (b) Photoemission-counts cross-section along the dashed line in a 3×3 point moving average of (a,top). (c) Topography cross-section along the dashed line in (a,bottom). The lighter regions in (a,bottom) correspond to apparent positions of Au as deposited in a Fischer pattern in the sample where the spheres were not closely packed. The remaining regions in (a,bottom) correspond to ITO. The STM parameters were as follows: V_s = 2.0 V, I = 0.6 nA, sampling time per point was 15ms. Scan resolution was 128×128 points.

Alternatively, if sudden increases in emission rate on Au never give rise to emission on ITO then, in conjunction with the results of sample type B, any contribution of a bright tip can be considered negligible or non-existent.

A typical example of such an experiment on sample type C is shown in Fig. 4. As given by Fig. 4(a), there is a good deal of line-to-line emission variability on the gold but there is no detectable signal on the ITO regions; the measured count rate on ITO is dark-count noise limited. A similar result has been shown in a different context by Uemura et al. [9]. Experiments on sample type C have been repeated with several tips on several samples at sample biases between 1.5 and 3 V, for both positive and negative polarity, and constant current set-points between 0.1 and 10 nA. At no time was photoemission observed on ITO regions, *even after* a brightening event. The cross-sections given by Figs. 4(b) and 4(c) give an example of the photoemission behavior immediately after such a brightening event. The emission rate on the gold increased by a factor of 6 relative to previous lines but count rates detected on ITO remain dark-count limited. This indicates that electroluminescent clusters are unlikely to contribute greatly to emission rates in STM experiments with Au tips on Au samples at ambient conditions.

In the absence of the bright-tip hypothesis, the conclusion can be made that plasmonic activity is responsible for the changes in the apparent emission rates shown in Fig. 2(a). In the top portion of Fig. 2(a) the emission rate appears to be roughly constant regardless of the sample topography. This leads to the conclusion that emission characteristics in this region are dominated by the tip because the emission does not appear to depend on the sample topography. After the abrupt change in the tip, as shown in Fig. 2(d) and corresponding to the bottom half of Fig. 2(a), the emission rate appears to vary greatly depending on the sample topography. This leads to the conclusion that the sample is dominating the emission characteristics in this region.

Based on the preceding conclusions and within the context of the findings by Mitra et al. with regard to gap plasmon modes [17], an interpretation can be made of the results shown in Fig. 2. In the tip-dominated top region only a single gap plasmon mode is active due to the

#195365 - $15.00 USD Received 6 Aug 2013; revised 21 Sep 2013; accepted 23 Sep 2013; published 4 Nov 2013

structure of the tip. Then an abrupt change in the tip occurs. The size of the tip appears to have increased as seen in comparing the apparent size of particles in the top and bottom portions of Fig. 2(c). This change allows for the simultaneous excitation of multiple gap plasmon modes. The number of excited modes can now depend on the local curvature of the sample as well as the tip. The flat areas in the sample allow for the excitation of a larger number of active gap modes than on the small particles and this leads to the difference in emission rates between the two as shown in the bottom portion of Fig. 2(a).

4. Conclusion

We have shown that the variability in STM photoemission rates between a gold tip and a gold film under ambient conditions is due entirely to the modification of the localized gap plasmon modes. While not an impossible source of photoemission in this context, electroluminescence from any gold clusters present in an STM junction operated at d.c. bias has been shown to be typically negligible. Further, we have found that photoemission can be significantly influenced not only by small-scale changes in the composition of the STM probe apex but also by relatively large topographical features such as 20 nm particles embedded beneath a gold film.

Acknowledgments

We sincerely thank the reviewers for their critical review of the original manuscript and for their detailed comments and questions. We thank M. Parzefall for helpful suggestions and for creating Fig. 1 of this paper. We also thank Z. Lapin and H. Scherrer for fruitful discussions. This project is funded by the Swiss National Science Foundation (SNF) through grant 200021_146358.

#195365 - $15.00 USD Received 6 Aug 2013; revised 21 Sep 2013; accepted 23 Sep 2013; published 4 Nov 2013